The Journal of Chemical Physics ARTICLE scitation.org/journal/jcp

Entropic surface segregation from athermal polymer blends: Polymer flexibility vs bulkiness

Cite as: J. Chem. Phys. 156, 184901 (2022); doi: 10.1063/5.0087587
Submitted: 7 February 2022 • Accepted: 21 April 2022 •
Published Online: 9 May 2022

M. W. Matsen[a]

AFFILIATIONS

Department of Chemical Engineering, Department of Physics & Astronomy, and Waterloo Institute for Nanotechnology, University of Waterloo, Waterloo, Ontario N2L 3G1, Canada

[a]Author to whom correspondence should be addressed: mwmatsen@uwaterloo.ca

ABSTRACT

We examine athermal binary blends composed of conformationally asymmetric polymers of equal molecular volume next to a surface of width ξ. The self-consistent field theory (SCFT) of Gaussian chains predicts that the more compact polymer with the shorter average end-to-end length, R_0, is entropically favored at the surface. Here, we extend the SCFT to worm-like chains with small persistence lengths, ℓ_p, relative to their contour lengths, ℓ_c, for which $R_0 \approx \sqrt{2\ell_p\ell_c}$. In the limit of $\ell_p \ll \xi$, we recover the Gaussian-chain prediction where the segregation depends only on the product $\ell_p\ell_c$, but for realistic polymer/air surfaces with $\xi \sim \ell_p$, the segregation depends separately on the two quantities. Although the surface continues to favor flexible polymers with smaller ℓ_p and bulky polymers with shorter ℓ_c, the effect of bulkiness is more pronounced. This imbalance can, under specific conditions, lead to anomalous surface segregation of the more extended polymer. For this to happen, the polymer must be bulkier and stiffer, with a stiffness that is sufficient to produce a larger R_0 yet not so rigid as to reverse the surface affinity that favors bulky polymers.

I. INTRODUCTION

Polymer surfaces are involved in many technological applications, including adhesion, lubrication, wetting, colloidal stabilization, catalysis, material processing, and protein adsorption.[1] For polymeric alloys (i.e., miscible blends), surface properties are largely dictated by the surface composition, which generally differs from that of the bulk due to surface segregation. Normally, the segregation is dominated by enthalpic considerations, but nevertheless there are significant entropic effects for high molecular-weight polymers. As such, the segregation behavior will be controlled by entropic effects when the enthalpic preferences are reasonably balanced.

One well established effect is the surface affinity for polymer ends,[2–7] which, in turn, favors the segregation of short polymers to a surface, given that they have more ends per unit volume of material.[8–12] In the case of branched architectures, the behavior becomes particularly interesting due to a competition between the ends that favor the surface and the junctions that disfavor the surface.[13,14] Even for polymers of the same architecture and molecular volume, surface segregation can also occur due to conformational differences between the polymers.

The effect of conformational asymmetry was first noticed by Sikka *et al.*[15,16] in experiments on a series of polyolefin diblock copolymers, where the two components were chemically similar but with considerably different statistical segment lengths. Note that the comparison is based on segments of equal molecular volume. The experiments observed that the diblock copolymers always ordered with the more compact (i.e., shorter statistical segment length) component at surfaces. Subsequent experiments by Scheffold *et al.*[17] on binary polyolefin blends found a similar preference for the more compact component. Other experiments by Tretinnikov and Ohta[18,19] examined blends of isotactic and syndiotactic PMMA, where the monomers are identical but linked together differently, resulting in a shorter statistical segment length for the syndiotactic polymer. Again, it was the more compact syndiotactic component that segregated to surfaces.

Self-consistent field theory (SCFT) calculations[20,21] of athermal blends involving polymers of identical molecular volume also found a surface affinity for the more compact component, consistent with the experiments. More specifically, SCFT predicts a positive surface excess,

$$\phi_{\rm ex}(z) \equiv \frac{1}{2}\big(\phi_2(z) - \bar{\phi}_2 - \phi_1(z) + \bar{\phi}_1\big), \tag{1}$$

provided that $R_{0,1} > R_{0,2}$. Here, $\phi_\gamma(z)$ and $\bar{\phi}_\gamma$ are the volume fractions of component γ at a distance z from the surface and in the bulk, respectively, and $R_{0,\gamma}$ is the average end-to-end length of γ-type polymer in the bulk. For small degrees of asymmetry, Wu *et al.*[21] showed that the excess takes the form

$$\phi_{\rm ex}(z) = A_\rho F_\rho(Z), \tag{2}$$

where the profile shape,

$$F_\rho(Z) = \frac{(1+Z^2)}{\sqrt{\pi}}\exp(-Z^2) - \left(\frac{3Z}{2} + Z^3\right)\mathrm{erfc}(Z), \tag{3}$$

is expressed in terms of $Z = \sqrt{3/2}z/\tilde{R}_0$, and the distance from the surface is scaled with respect to the average size of the polymers,

$$\tilde{R}_0^2 \equiv \frac{1}{2}\left(R_{0,1}^2 + R_{0,2}^2\right). \tag{4}$$

Furthermore, they showed that the amplitude scales as

$$A_\rho \propto \bar{\phi}_1\bar{\phi}_2\Delta R_0/\xi, \tag{5}$$

where ξ is the width of the surface and

$$\Delta R_0 \equiv R_{0,1} - R_{0,2} \tag{6}$$

measures the conformational asymmetry.

Likewise, simulations for diblock copolymers[22] and for polymer blends[23,24] are in general agreement with the experiments. Although some simulations[25,26] initially predicted a surface preference for stiffer polymers, this has recently been attributed to insufficient equilibration and statistics.[24] Interestingly, the surface excesses predicted by the simulations in Refs. 23 and 24 conform to Eq. (3), provided that the conformational asymmetry is not too large. Given that $F_\rho(Z)$ in Eq. (3) was derived for Gaussian chains, the fact that it agrees with different simulation models suggests that it is a universal profile that applies to all models. If so, it must then also apply to experiments, given that models can, in principle, be refined to be arbitrarily accurate. On the other hand, the amplitude of the excess, A_ρ, does depend on the details of the system and, thus, will not necessarily follow the predicted scaling in Eq. (5).

Carignano and Szleifer[27] have, in fact, illustrated that entropic surface segregation is not solely dictated by differences in R_0. They did so by modeling diblock copolymers and polymer blends using semi-flexible polymers, where conformational asymmetry can result from a mismatch in flexibility (i.e., persistence length) and/or a mismatch in bulkiness (i.e., contour length). Note that the fixed molecular volume of the polymers requires the contour length of a polymer to be inversely proportional to its cross-sectional area, which is a measure of bulkiness. Interestingly, Carignano and Szleifer not only showed that the two types of conformational asymmetry are not equivalent but also found that the behavior was not even qualitatively the same in the case of polymer blends. However, some of the difference might be due to computational inaccuracies resulting from the inefficiency of their mean-field type calculation.

Efficient mean-field calculations (i.e., SCFT) are able to consider all possible conformations of a polymer molecule by using propagators or rather partial partition functions.[28] The calculations by Carignano and Szleifer, on the other hand, were limited to 10^7 randomly generated conformations, which amounts to a tiny sample of the total population. Given that polymer conformations near a surface are not typical of those in the bulk, it is conceivable that the sample did not contain a sufficient number of representative conformations. Not only this, the computational cost of their approach limited their study to thin films. Here, these shortcomings are avoided with the use of SCFT calculations for worm-like chains.[28–31] Our focus will be on binary blends with small degrees of conformational asymmetry, for which the excess should obey Eq. (2).

II. THEORY

The specific system of our study is an athermal binary blend of n_1 polymers of contour length $\ell_{c,1}$ and persistence length $\ell_{p,1}$ mixed with n_2 polymers of contour length $\ell_{c,2}$ and persistence length $\ell_{p,2}$. From these quantities, we define average values and differences as

$$\bar{\ell}_\alpha \equiv \frac{1}{2}(\ell_{\alpha,1} + \ell_{\alpha,2}), \tag{7}$$

$$\Delta\ell_\alpha \equiv \ell_{\alpha,1} - \ell_{\alpha,2}, \tag{8}$$

respectively. Both polymer species are assumed to have identical numbers of segments, N, each of volume ρ_0^{-1}. Hence, the polymers are of equal molecular volume, and as such, they will not be affected by entropic segregation due to size disparity. As previously stated, the polymers will be modeled as worm-like chains, for which the average end-to-end lengths in the bulk are given by[28]

$$R_{0,\gamma} = \left[2\ell_{p,\gamma}\ell_{c,\gamma} - 2\ell_{p,\gamma}^2\left(1 - e^{-\ell_{c,\gamma}/\ell_{p,\gamma}}\right)\right]^{1/2}. \tag{9}$$

We will focus on relatively flexible polymers (i.e., $\ell_{c,\gamma} \gg \ell_{p,\gamma}$), in which case the expression reduces to

$$R_{0,\gamma} \approx \sqrt{2\ell_{p,\gamma}\ell_{c,\gamma}}. \tag{10}$$

This implies that the statistical segment lengths are

$$a_\gamma \equiv \frac{R_{0,\gamma}}{\sqrt{N}} = \sqrt{2\ell_{p,\gamma}b_\gamma}, \tag{11}$$

where $b_\gamma \equiv \ell_{c,\gamma}/N$ is the contour length of an individual segment.

We are interested in a semi-infinite melt next to a flat surface at $z = 0$, which is achieved by extending the system to a sufficient distance, $z \le L$, to reach bulk-like conditions. To make the problem tractable, the molecular interactions are represented by a static field, $w(z)$, which depends only on the distance from the surface. The segregation is determined by calculating the local volume fraction of the γ-type polymers,

$$\phi_\gamma(z) = \frac{1}{2}\int_{-1}^{1} du_z p_\gamma(z, u_z), \tag{12}$$

which is expressed in terms of the probability density, $p_\gamma(z, u_z)$, of finding a segment of type γ at position z with orientation $u_z = \cos(\theta)$. In the canonical ensemble, the joint distribution is given by

$$p_\gamma(z, u_z) = \frac{n_\gamma L}{nQ_\gamma}\int_0^1 ds\, G_\gamma(z, u_z, s)G_\gamma(z, -u_z, 1-s), \tag{13}$$

where $n = n_1 + n_2$ is the total number of polymers and

$$Q_\gamma = \frac{1}{2}\int_{-1}^{1} du_z \int dz\, G_\gamma(z, u_z, s) G_\gamma(z, -u_z, 1-s) \tag{14}$$

is a single-chain partition function. These expressions involve a partial partition function, $G_\gamma(z, u_z, s)$, for a length $s\ell_{c,\gamma}$ of γ-type polymer, where one end is constrained at a distance z from the surface with orientation u_z. The partial partition function satisfies the differential equation

$$\frac{\partial G_\gamma}{\partial s} = \frac{\ell_{c,\gamma}}{2\ell_{p,\gamma}} \frac{\partial}{\partial u_z}\left[(1-u_z^2)\frac{\partial G_\gamma}{\partial u_z}\right] - \ell_{c,\gamma} u_z \frac{\partial G_\gamma}{\partial z} - w G_\gamma, \tag{15}$$

subject to the initial condition $G_\gamma(z, u_z, 0) = 1$.[28] The differential equation is solved with reflecting boundary conditions [e.g., $G_\gamma(L+\varepsilon, u_z, s) = G_\gamma(L-\varepsilon, -u_z, s)$] using the numerical algorithm described in Ref. 31.

Here, we create the surface by adjusting the field, $w(z)$, so that the total polymer concentration conforms to the sigmoidal profile,

$$\phi_1(z) + \phi_2(z) = \frac{1}{2}\left[1 + \tanh\left(\frac{2z}{\xi}\right)\right], \tag{16}$$

which is characteristic of simulations.[32,33] The width of the surface, ξ, serves as our unit of length. Equation (16) is solved by iterating the field with the same Anderson mixing algorithm[34] used previously.[6,7,10] For simplicity, we limit our attention to balanced blends with a 50-50 composition, and therefore, we start by solving the field equation for $n_1 = n_2$. However, as a consequence of our finite system size, the surface segregation causes a small deviation from 50-50 composition in the bulk (i.e., near $z = L$). This could be remedied by switching to a grand-canonical ensemble,[6,10] but that reduces the stability of the Anderson mixing algorithm. Therefore, we instead adjust the composition iteratively,

$$n_1 \to \frac{n_1}{2\phi_1(L)} \quad \text{with} \quad n_2 = n - n_1, \tag{17}$$

until a 50-50 bulk composition is obtained. An accurate balance is typically achieved in one or two iterations of n_γ. Note that we always ensure that the numerical inaccuracy in our calculated quantities is negligible on the scale of our plots.

We also perform a few calculations for Gaussian polymers. The calculations are essentially the same as for worm-like polymers, except that the partial partition function, $G_\gamma(z, s)$, no longer depends on the chain orientation, u_z. As a consequence, it satisfies the simpler differential equation,

$$\frac{\partial G_\gamma}{\partial s} = \frac{R_{0,\gamma}^2}{6}\frac{\partial^2 G_\gamma}{\partial z^2} - w G_\gamma, \tag{18}$$

with the initial condition $G_\gamma(z, 0) = 1$.[28] In this case, the differential equation is solved using the standard Crank–Nicolson algorithm.

III. RESULTS

For comparison purposes, we begin by considering the Gaussian-chain limit (i.e., $\ell_p \to 0$ and $\ell_c \to \infty$). Figure 1 plots the concentration profiles for a 50-50 blend of polymers with a small conformational asymmetry corresponding to $R_{0,1} = 30.3\xi$ and $R_{0,2} = 29.7\xi$. Consistent with previous SCFT calculations,[20,21] the more compact component with the smaller statistical segment length (i.e., $\gamma = 2$) segregates to the surface. The inset shows that the excess at the surface reaches 8% even though the relative difference in statistical segment lengths is just 2%.

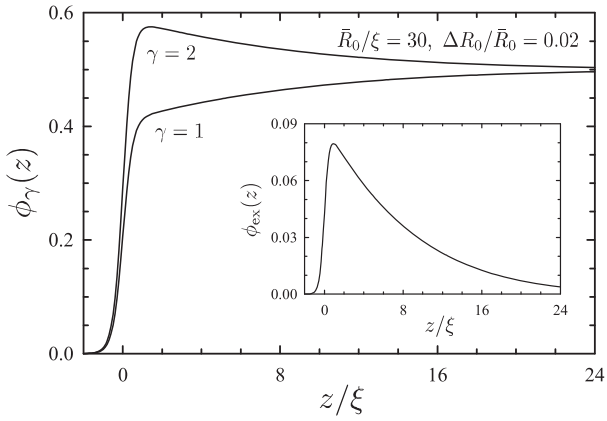

FIG. 1. Concentration profiles, $\phi_\gamma(z)$, for an athermal binary blend of Gaussian polymers with an average end-to-end length of $\bar{R}_0/\xi = 30$ and a conformational asymmetry of $\Delta R_0/\bar{R}_0 = 0.02$ next to a surface of width ξ at $z = 0$. The inset shows the excess concentration of the more compact component with the shorter statistical segment length.

Figure 2(a) goes on to compare the excesses for blends with average end-to-end lengths of $\bar{R}_0 = 20$, 30, and 40 and relative conformational asymmetries of $\Delta R_0/\bar{R}_0 = 0.01$ and 0.02. As expected, the amplitude increases for larger conformational asymmetry and the range extends further for larger polymers. Consistent with Eq. (2), the profiles collapse when $\phi_{ex}(z)$ is scaled by $\Delta R_0/\xi$ and z is scaled by $\bar{R}_0$, as demonstrated in Fig. 2(b). The dashed curve corresponds to the fit

$$A_\rho = 0.27\frac{\Delta R_0}{\xi}, \tag{19}$$

which is the same scaling predicted by Wu *et al.*[21] The prefactor of 0.27 is different, but that is just because our surface profile has a different shape [Eq. (16)].

We now turn our attention to worm-like chains, starting with blends for which the conformational asymmetries arises solely from a difference in bulkiness. For this, we set both persistence lengths equal to twice the width of the surface (i.e., $\Delta\ell_p = 0$ and $\bar{\ell}_p = 2\xi$). We then select $\bar{\ell}_c$ to match the $\bar{R}_0$ values in Fig. 2 using Eq. (10) and $\Delta\ell_c$ to match the conformational asymmetry using $\Delta R_0/\bar{R}_0 \approx \frac{1}{2}\Delta\ell_c/\bar{\ell}_c$, which follows immediately from the relationship in Eq. (10). The results for worm-like polymers, plotted in Fig. 3(a), are virtually identical to those for the Gaussian polymers, plotted in Fig. 2(a), except that the excesses are now reduced by about 40%. As before, the data collapse when the excesses are scaled by

$$\frac{\Delta R_0}{\xi} \approx \frac{\bar{R}_0}{2\xi}\frac{\Delta\ell_c}{\bar{\ell}_c} = \frac{\Delta\ell_c}{\xi^{1/2}\bar{\ell}_c^{\,1/2}}, \tag{20}$$

as confirmed by Fig. 3(b).

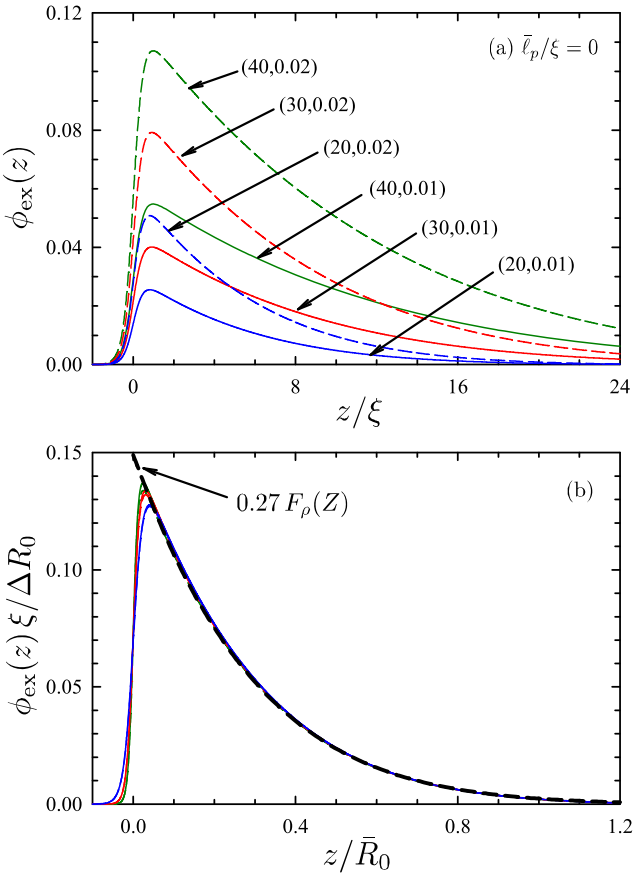

FIG. 2. (a) Excess concentrations, $\phi_{ex}(z)$, for blends of Gaussian polymers with a selection of different $\bar{R}_0/\xi$ and $\Delta R_0/\bar{R}_0$ values; curves are labeled by $(\bar{R}_0/\xi, \Delta R_0/\bar{R}_0)$. (b) Scaled plot of the same data fit to $F_\rho(Z)$ in Eq. (3).

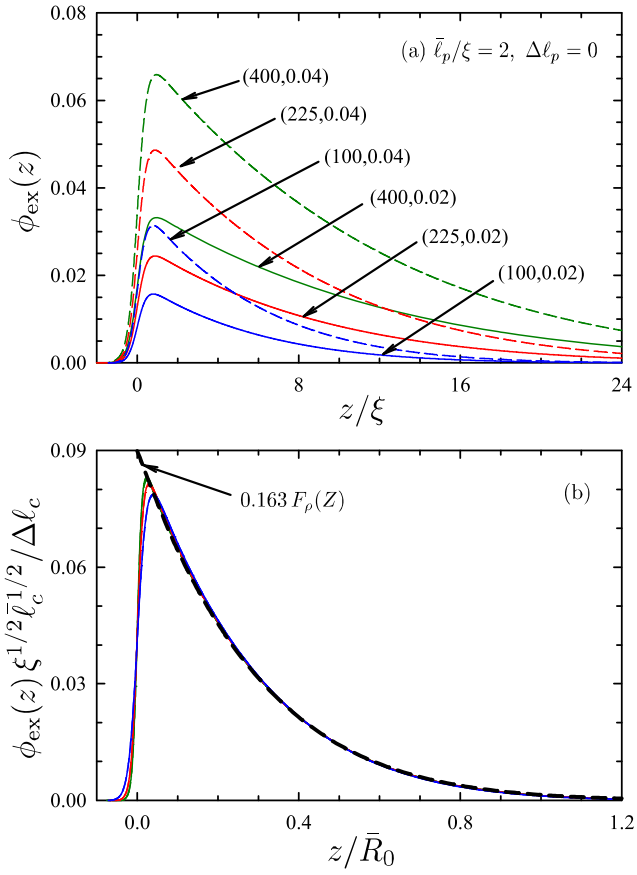

FIG. 3. (a) Excess concentration, $\phi_{ex}(z)$, for blends of worm-like polymers with $\bar{\ell}_p/\xi = 2$, $\Delta\ell_p = 0$, and a selection of different $\bar{\ell}_c$ and $\Delta\ell_c$ values; curves are labeled by $(\bar{\ell}_c/\xi, \Delta\ell_c/\bar{\ell}_c)$. (b) Scaled plot of the same data fit to $F_\rho(Z)$.

Next, we perform equivalent calculations for blends of worm-like polymers with conformational asymmetries arising solely from a difference in flexibility. For this, we consider the same series of $\bar{\ell}_p$ and $\bar{\ell}_c$ values as in Fig. 3(a) but now with $\Delta\ell_c = 0$ and $\Delta\ell_p \neq 0$. The results shown in Fig. 4(a) are again analogous to those in Fig. 2(a) for Gaussian polymers, except that this time the excesses are reduced by ~70%. Similarly, the data collapse when scaled with respect to

$$\frac{\Delta R_0}{\xi} \approx \frac{\bar{R}_0}{2\xi}\frac{\Delta\ell_p}{\bar{\ell}_p} = \frac{\bar{\ell}_c^{\,1/2}\Delta\ell_p}{2\xi^{3/2}}, \tag{21}$$

as demonstrated in Fig. 4(b).

Provided that the conformational asymmetry is small, the first-order effects of $\Delta\ell_c$ and $\Delta\ell_p$ should be additive. Hence, we expect the amplitude of the excess to scale as

$$A_\rho \approx 0.27\frac{\bar{R}_0}{2\xi}\left(f_c\frac{\Delta\ell_c}{\bar{\ell}_c} + f_p\frac{\Delta\ell_p}{\bar{\ell}_p}\right), \tag{22}$$

where the coefficients f_c and f_p depend on the average persistence length, $\bar{\ell}_p$. Note that the prefactor of 0.27 from Eq. (19) is inserted so that $f_c = f_p = 1$ in the Gaussian-chain limit of $\bar{\ell}_p = 0$. Based on the fits in Figs. 3(b) and 4(b), the coefficients are reduced to $f_c = 0.600$ and $f_p = 0.298$ for a non-zero persistence length of $\bar{\ell}_p = 2\xi$. The full dependences of f_c and f_p on $\bar{\ell}_p$, plotted in Fig. 5, are obtained by repeating the fits for different average persistence lengths. Note that the coefficients satisfy the inequality $f_p < f_c$, which implies that the surface affinity for bulky polymers due to $\Delta\ell_c \neq 0$ generally dominates the surface affinity for flexible polymers due to $\Delta\ell_p \neq 0$.

To confirm the linearity of Eq. (22), Fig. 6 plots contours of constant A_ρ as a function of $\Delta\ell_c$ and $\Delta\ell_p$ for blends with $\bar{\ell}_c = 225\xi$ and $\bar{\ell}_p = 2\xi$ (i.e., $\bar{R}_0 = 30\xi$). Indeed, the contours are almost perfectly linear. The slope of the contours illustrates again that A_ρ has a stronger dependence on $\Delta\ell_c$ than on $\Delta\ell_p$, which has an interesting implication. Consider the dashed line in Fig. 6, which corresponds to a conformational asymmetry of $\Delta R_0/\bar{R}_0 = 0.02$. For flexible Gaussian polymers, the amplitude of the excess would maintain the fixed value of $A_\rho = 0.16$ from Fig. 1 along the entire line. However, for

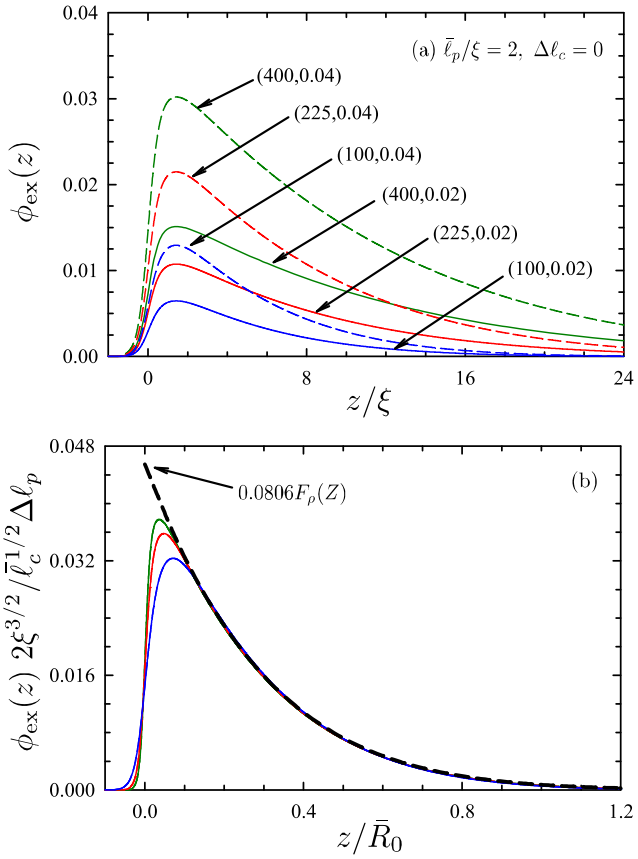

FIG. 4. (a) Excess concentration, $\phi_{ex}(z)$, for blends of worm-like polymers with $\bar{\ell}_p/\xi = 2$, $\Delta\ell_c = 0$, and a selection of different $\bar{\ell}_c$ and $\Delta\ell_p$ values; curves are labeled by $(\bar{\ell}_c/\xi, \Delta\ell_p/\bar{\ell}_p)$. (b) Scaled plot of the same data fit to $F_\rho(Z)$.

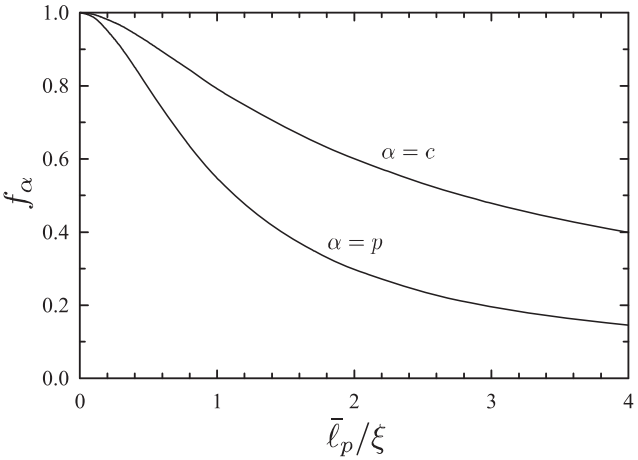

FIG. 5. Coefficients in Eq. (22) for the amplitude of the entropic segregation, A_ρ, plotted as a function of average persistent length, $\bar{\ell}_p$.

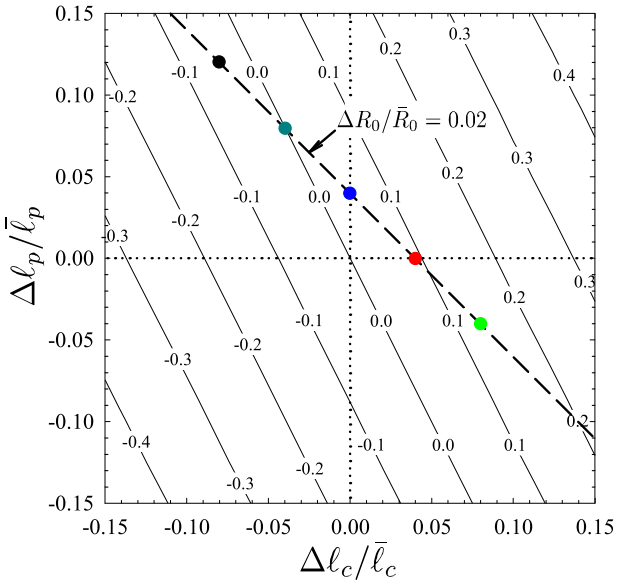

FIG. 6. Amplitude of the surface excess, A_ρ, for blends of worm-like polymers with $\bar{\ell}_c/\xi = 225$ and $\bar{\ell}_p/\xi = 2$ plotted as a function of the asymmetries $\Delta\ell_c$ and $\Delta\ell_p$. The dashed line corresponds to an equivalent asymmetry, $\Delta R_0/\bar{R}_0 = 0.02$, to that of the Gaussian polymers in Fig. 1.

semi-flexible worm-like polymers, A_ρ varies according to the type of conformational asymmetry (i.e., bulkiness vs flexibility). In fact, A_ρ can even become negative, resulting in anomalous surface segregation of the more extended polymer with the larger statistical segment length.

Figure 7(a) plots the surface excess, $\phi_{ex}(z)$, at the five points marked along the dashed line in Fig. 6. Given the dominating effect of bulkiness, the amplitude of the excess correlates most closely with $\Delta\ell_c/\bar{\ell}_c$. As such, A_ρ reverses sign once $\Delta\ell_c/\bar{\ell}_c$ becomes sufficiently negative, resulting in the anomalous behavior where the more extended polymer segregates to the surface. Even still, Fig. 7(b) demonstrates that the profile shape, $F_\rho(Z)$, remains universal regardless of the sign of A_ρ. The excess does, however, deviate from the universal profile for $A_\rho \approx 0$, and therefore, we have omitted the curve for $\Delta\ell_c/\bar{\ell}_c = -0.04$ from Fig. 7(b).

Interestingly, the excess for $\Delta\ell_c/\bar{\ell}_c = -0.08$, corresponding to the anomalous segregation, exhibits a pronounced short-range contribution in addition to the long-range excess of $A_\rho F_\rho(Z)$. This is particularly evident in Fig. 7(b). We attribute this effect to the ability of stiffer polymers to align with the surface due to the fact that they have less conformational entropy. To illustrate this, Fig. 8 plots the orientational order parameters,

$$S_\gamma(z) = \frac{1}{2\phi_\gamma(z)} \int_{-1}^{1} du_z P_2(u_z) p_\gamma(z, u_z), \tag{23}$$

of the two polymers ($\gamma = 1$ and 2), where $P_2(x) = (3x^2 - 1)/2$ is the second Legendre polynomial. The order parameters vary from $-1/2$ for perfect orientation parallel to the surface to $+1$ for perfect orientation normal to the surface. Although both polymers tend to align parallel to the surface around $z \approx 0.4\xi$, consistent with simulations[23]

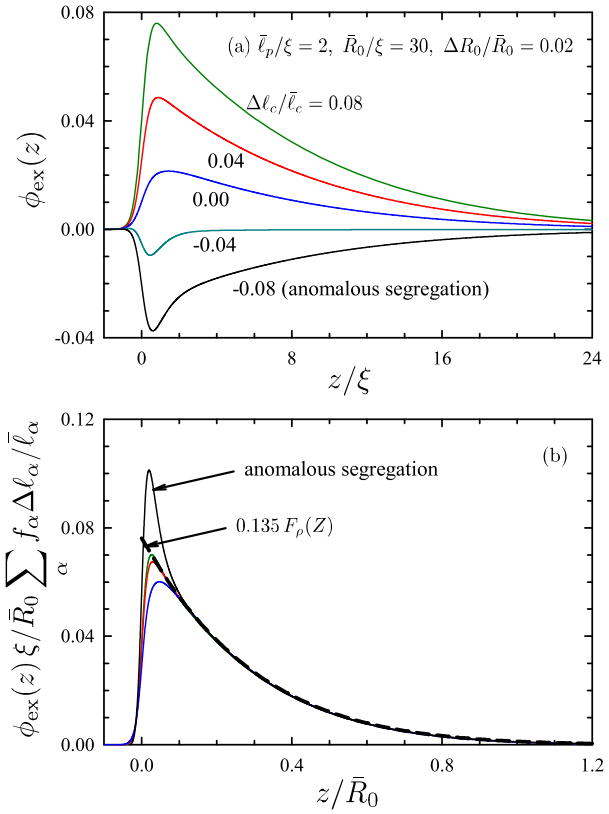

FIG. 7. (a) Surface excess, $\phi_{ex}(z)$, for blends corresponding to the five points along the dashed line in Fig. 6. (b) Scaled plot of the same data (apart from $\Delta\ell_c/\bar{\ell}_c = -0.04$) fit to $F_\rho(Z)$.

and SCFT,[30] the alignment is stronger for the stiffer polymers, as suspected. Note that the positive value of $S_\gamma(z)$ at negative z can be attributed to chain ends sticking out of the surface, which was also observed in simulations.[23]

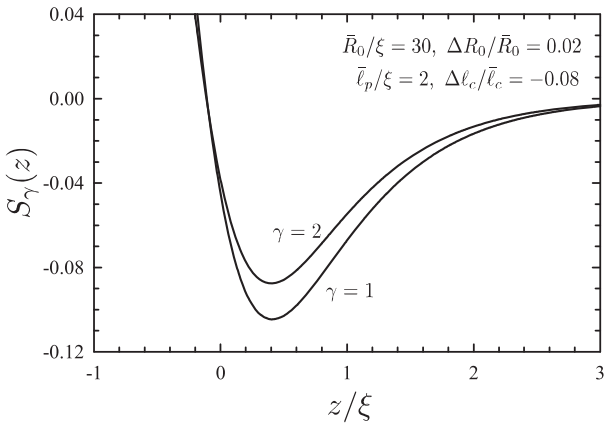

FIG. 8. Orientational order parameters, $S_\gamma(z)$, for the anomalous segregation in Fig. 7, where the more extended polymer ($\gamma = 1$) segregates to the surface.

IV. DISCUSSION

Naturally, the mean-field approximation of SCFT will result in some degree of inaccuracy. For instance, it neglects the packing effects responsible for layering near solid surfaces[23,25,26,32] and nematic-type ordering among neighboring polymers.[24,35] Kumar *et al.*[26] suggested that these packing effects are essential for a proper treatment of surface segregation, but the simulations and wall-PRISM calculations supporting this claim are now known to be incorrect.[23] In any case, the packing effects should be relatively minor at polymer/air surfaces where the layering is generally absent.[32] Furthermore, the onset of nematic order generally requires a considerable degree of rigidity well beyond that of typical polymers.[23] Thus, there is every reason to expect the mean-field approximation to be reliable for the conditions of our study.

A more serious approximation in SCFT calculations, however, is the use of the Gaussian-chain model.[20,21] For it to be accurate, the persistence length, ℓ_p, of the polymers needs to be small relative to all relevant length scales, including the width of the surface, ξ. While this is generally true for polymer/polymer interfaces,[30] polymer/air surfaces are considerably narrower. Consequently, even relatively flexible polymers do not generally satisfy the necessary criterion, $\ell_p \ll \xi$. This was, in fact, our motivation for extending the previous SCFT calculations to worm-like polymers.

The SCFT calculation by Wu *et al.*[21] derived the analytical results in Eqs. (2), (3), and (5) by separating the problem into an inner part, $z \lesssim \xi$, and an outer part, $z \gtrsim \xi$. The outer solution deals with how the perturbation of the surface relaxes to bulk conditions. As such, the profile, $F_\rho(Z)$, originates from the Debye function for ideal Gaussian polymers.[21] In this case, the relevant length scale is $\bar{R}_0$, which is generally much larger than ℓ_p. It is for this reason that $F_\rho(Z)$ remains valid for our worm-like polymers. Likewise, this is why the simulations in Refs. 23 and 24 observe the same profile despite the use of different models and why the profile should also apply to experiments.

The amplitude of the excess, A_ρ, is determined by matching the inner and outer solutions. Since the inner solution is sensitive to the details of the system, the same must be true of A_ρ. Hence, Eq. (5) is not expected to hold in general, and in particular, conformational asymmetry will not be dictated solely by differences in the average end-to-end lengths, ΔR_0. Just as Carignano and Szleifer[27] argued, the excess will depend on whether ΔR_0 results from a difference in bulkiness or flexibility. Although they correctly anticipated the distinct behavior, their predictions were almost certainly affected by the inefficiency of their mean-field approach. Contrary to their claims, we find that both effects still produce a surface affinity for the more compact polymer with the smaller statistical segment length. It is just that bulkiness has a stronger effect than flexibility.

The fact that the effect of bulkiness is more pronounced sets up the possibility of anomalous segregation, where the more extended polymer is favored at the surface. For this to happen, the polymer must be bulkier with an appropriate degree of stiffness. In particular, the stiffness has to be sufficient for the polymer to be more extended but not so large as to dominate the surface segregation. For our previous example of $\Delta\ell_c/\bar{\ell}_c = -0.08$ and $\bar{\ell}_p/\xi = 2$ (see Fig. 6), the stiffness disparity must fall within the interval $0.08 \lesssim \Delta\ell_p/\bar{\ell}_p \lesssim 0.16$ in order to produce a negative A_ρ with a positive ΔR_0.

There is one notable difference in our treatment of the surface from that of the previous SCFT calculations.[20,21] We simply assume the sigmoidal profile in Eq. (16), whereas the previous calculations created the surface by incorporating the interaction energy,

$$U = \frac{1}{2\kappa} \int d\mathbf{r}[\phi_1(z) + \phi_2(z)]^2, \tag{24}$$

where κ is a dimensionless compressibility. By doing so, they were able to express ξ in terms of κ, but unfortunately the resulting behavior proves to be unphysical. For instance, the surface narrows as N is decreased,[4] which contradicts the common-sense behavior observed in simulations.[32] Furthermore, the concentration profile deviates from the sigmoidal shape observed in simulations of polymer/air surfaces.[32,33]

Although the interaction energy in Eq. (24) is appropriate for small deviations from bulk concentration [i.e., $\phi_1(z) + \phi_2(z) \approx 1$], it breaks down for surfaces where the concentration drops to zero. The formation of a polymer/air surface requires cohesive interactions balanced by hard-core interactions. The choice of U in Eq. (24), however, corresponds to purely repulsive interactions, which cause the polymers to behave like a gas that fills all available space. To contain the polymers, U needs to be supplemented by a Dirichlet boundary condition, which amounts to imposing a hard wall. The problem could be circumvented by incorporating a density functional approach,[36–39] which if accurate would produce a sigmoidal-like profile. However, the only thing gained by such an approach is that the width of the surface, ξ, can then be expressed in terms of the parameters of the density functional theory, which, in turn, would be related to the molecular parameters of the system. Other than that, we obtain the same results by simply assuming the appropriate profile shape.

Given that our concentration profile in Eq. (16) is characteristic of polymer/air surfaces, our results will be less relevant to polymer/solid surfaces. Furthermore, solid surfaces will amplify the packing effects ignored by SCFT, as mentioned above. Nevertheless, the behavior is likely to remain much the same. For instance, the $F_\rho(Z)$ profile in Eq. (3) will still apply,[23,24] since it is unaffected by the surface details.[4] The scaling of A_ρ in Eq. (22) may also remain the same, although there are bound to be considerable changes to the prefactor, 0.27, and the coefficients, f_c and f_p. However, we still expect that inequality $f_c > f_p$ to hold, and thus, the asymmetry in bulkiness will presumably continue to dominate the asymmetry in flexibility.

One limitation of our coarse-grained model is that it does not account for the molecular structure responsible for bulkiness (i.e., short-fat polymers as opposed to long-thin polymers). In real systems, such as polyolefins,[15–17] bulkiness typically results from the presence of side units. Their size and spacing, for example, will affect the local surface behavior and, therefore, impact the amplitude, A_ρ, of the long-range excess. While these effects are presumably small, they are also beyond the capabilities of our SCFT approach. Although one can, in principle, incorporate side units into the model,[28] there would be no point in doing so. The mean-field approximation is simply not accurate enough to justify such refinements.

Yethiraj[40] actually performed simulations of linear polymers and branched polymers with explicit side units, and Tripathi and Chapman[41] corroborated some of the predictions using density functional theory (DFT). Although the simulations are specific to polymer/solid surfaces, Yethiraj was able to alter the surface profile by including neutral (i.e., unbiased) interactions. The broader profiles resulted in a considerable surface affinity for the branched polymer with the shorter statistical segment length, but this preference reversed for the sharper profiles. Notably, none of the results seem to conform to the universal profile, but this could be due to the low degree of polymerization ($N = 19$). More concerning is the fact that, in some cases, the excesses extended well beyond $\tilde{R}_0$. There are, in fact, a number of issues with the simulations. First, low polymerization is unlikely to produce significant polymeric effects. Second, the polymer concentration is also low, which can lead to unrealistic profiles where the surface concentration far exceeds the bulk concentration.[23,24] Third, the model and the number of Monte Carlo steps are similar to those of Refs. 25 and 26, which proved to be inaccurate due to insufficient equilibration and statistics, even for $N = 10$.[24] Although the simulations of Ref. 40 are supported by DFT, the latter simulations were likewise supported by wall-PRISM calculations. Needless to say, it would be useful to revisit these simulations.

V. SUMMARY

We have extended the previous SCFT calculations for entropic surface segregation[20,21] from Gaussian polymers to worm-like polymers. To avoid the need for realistic molecular interactions, we simply impose a sigmoidal concentration profile [Eq. (16)], which is characteristic of polymer/air surfaces.[32,33] The persistence lengths of our polymers, $\ell_{p,1}$ and $\ell_{p,2}$, are comparable to the width of the surface, ξ, but much smaller than the contour lengths of the polymers, $\ell_{c,1}$ and $\ell_{c,2}$. To isolate entropic effects due to conformational asymmetry, the polymers were assigned equal molecular volumes and the Flory–Huggins interaction parameter, χ, was set to zero. Unlike for the Gaussian chain model, where the conformational asymmetry arises solely from a difference in end-to-end lengths, ΔR_0, the worm-like chain model has two distinct sources of asymmetry: the difference in flexibility (i.e., $\Delta\ell_p \equiv \ell_{p,1} - \ell_{p,2}$) and the difference in bulkiness (i.e., $\Delta\ell_c \equiv \ell_{c,1} - \ell_{c,2}$).

The worm-like model still predicts a general surface affinity for the more compact polymer with the smaller persistence length and/or shorter contour length. Provided that the conformational asymmetry is not too large, the surface excess, $\phi_{ex}(z)$, continues to conform to the universal profile, $F_\rho(Z)$, in Eq. (3) predicted for Gaussian polymers,[21] but the amplitude of the excess, A_ρ, no longer obeys the simple scaling in Eq. (5). Instead of just depending on the difference in the end-to-end lengths, ΔR_0, it depends separately on the differences in flexibility, $\Delta\ell_p$, and in bulkiness, $\Delta\ell_c$, as specified by Eq. (22). The strengths of the two effects, f_c and f_p, both diminish as the average persistence length, $\tilde{\ell}_p$, increases (see Fig. 5). However, f_c remains larger than f_p, which implies that the segregation is affected by the bulkiness more than the flexibility of the polymers. As such, anomalous surface segregation of the more extended polymer can occur under appropriate conditions. In particular, the polymer has to be bulkier with a sufficient stiffness to produce a larger end-to-end length but not so much as to reverse the segregation effect due to bulkiness. Naturally, it would be interesting to test these predictions with simulations.

AUTHOR DECLARATIONS

Conflict of Interest

The authors have no conflicts to disclose.

DATA AVAILABILITY

The data that support the findings of this study are available from the corresponding author upon reasonable request.

REFERENCES

[1] K. Binder, "Surface effects on polymer blends and block copolymer melts: Theoretical concepts of surface enrichment, surface induced phase separation and ordering," Acta Polym. **46**, 204–225 (1995).

[2] I. Bitsanis and G. Hadziioannou, "Molecular dynamics simulations of the structure and dynamics of confined polymer melts," J. Chem. Phys. **92**, 3827–3847 (1990).

[3] W. Zhao, X. Zhao, M. H. Rafailovich, J. Sokolov, R. J. Composto, S. D. Smith, T. P. Russell, W. D. Dozier, T. Mansfield, and M. Satkowski, "Segregation of chain ends to polymer melt surfaces and interfaces," Macromolecules **26**, 561–562 (1993).

[4] D. T. Wu, G. H. Fredrickson, J.-P. Carton, A. Ajdari, and L. Leibler, "Distribution of chain ends at the surface of a polymer melt: Compensation effects and surface tension," J. Polym. Sci., Part B: Polym. Phys. **33**, 2373–2389 (1995).

[5] R. S. Pai-Panandiker, J. R. Dorgan, and T. Pakula, "Static properties of homopolymer melts in confined geometries determined by Monte Carlo simulation," Macromolecules **30**, 6348–6352 (1997).

[6] P. Mahmoudi and M. W. Matsen, "Segregation of chain ends to the surface of a polymer melt: Effect of surface profile versus chain discreteness," Eur. Phys. J. E **39**, 78 (2016).

[7] S. Blaber, P. Mahmoudi, R. K. W. Spencer, and M. W. Matsen, "Effect of chain stiffness on the entropic segregation of chain ends to the surface of a polymer melt," J. Chem. Phys. **150**, 014904 (2019).

[8] A. Hariharan, S. K. Kumar, and T. P. Russell, "A lattice model for the surface segregation of polymer chains due to molecular weight effects," Macromolecules **23**, 3584–3592 (1990).

[9] V. S. Minnikanti, Z. Qian, and L. A. Archer, "Surface segregation and surface tension of polydisperse polymer melts," J. Chem. Phys. **126**, 144905 (2007).

[10] P. Mahmoudi and M. W. Matsen, "Entropic segregation of short polymers to the surface of a polydisperse melt," Eur. Phys. J. E **40**, 85 (2017).

[11] P. Mahmoudi, W. S. R. Forrest, T. M. Beardsley, and M. W. Matsen, "Testing the universality of entropic segregation at polymer surfaces," Macromolecules **51**, 1242–1247 (2018).

[12] J. A. Hill, K. J. Endres, P. Mahmoudi, M. W. Matsen, C. Wesdemiotis, and M. D. Foster, "Detection of surface enrichment driven by molecular weight disparity in virtually monodisperse polymers," ACS Macro Lett. **7**, 487–492 (2018).

[13] D. T. Wu and G. H. Fredrickson, "Effect of architecture in the surface segregation of polymer blends," Macromolecules **29**, 7919–7930 (1996).

[14] V. S. Minnikanti and L. A. Archer, "Entropic attraction of polymers toward surfaces and its relationship to surface tension," Macromolecules **39**, 7718–7728 (2006).

[15] M. Sikka, N. Singh, A. Karim, F. S. Bates, S. K. Satija, and C. F. Majkrzak, "Entropy-driven surface segregation in block copolymer melts," Phys. Rev. Lett. **70**, 307–310 (1993).

[16] M. Sikka, N. Singh, F. S. Bates, A. Karim, S. Satija, and C. F. Majkrzak, "Surface segregation in model symmetric polyolefin diblock copolymer melts," J. Phys. II **4**, 2231–2248 (1994).

[17] F. Scheffold, A. Budkowski, U. Steiner, E. Eiser, J. Klein, and L. J. Fetters, "Surface phase behavior in binary polymer mixtures. II. Surface enrichment from polyolefin blends," J. Chem. Phys. **104**, 8795–8806 (1996).

[18] O. N. Tretinnikov and K. Ohta, "Surface segregation in stereochemically asymmetric polymer blends," Langmuir **14**, 915–920 (1998).

[19] O. N. Tretinnikov, "Surface segregation in polymer blends of minimal difference in the components surface energy," Macromol. Symp. **149**, 269–275 (2000).

[20] J. P. Donley and G. H. Fredrickson, "Influence of conformational asymmetry on the surface enrichment of polymer blends II," J. Polym. Sci., Part B: Polym. Phys. **33**, 1343–1351 (1995).

[21] D. T. Wu, G. H. Fredrickson, and J. P. Carton, "Surface segregation in conformationally asymmetric polymer blends: Incompressibility and boundary conditions," J. Chem. Phys. **104**, 6387–6397 (1996).

[22] A. Nikoubashman, R. A. Register, and A. Z. Panagiotopoulos, "Sequential domain realignment driven by conformational asymmetry in block copolymer thin films," Macromolecules **47**, 1193–1198 (2014).

[23] R. K. W. Spencer and M. W. Matsen, "Surface segregation in athermal polymer blends due to conformational asymmetry," Macromolecules **54**, 10100–10109 (2021).

[24] R. K. W. Spencer and M. W. Matsen, "Universality of entropic surface segregation from athermal polymer blends due to conformational asymmetry," Macromolecules **55**, 1120–1126 (2022).

[25] A. Yethiraj, S. Kumar, A. Hariharan, and K. S. Schweizer, "Surface segregation in polymer blends due to stiffness disparity," J. Chem. Phys. **100**, 4691–4694 (1994).

[26] S. K. Kumar, A. Yethiraj, K. S. Schweizer, and F. A. M. Leermakers, "The effects of local stiffness disparity on the surface segregation from binary polymer blends," J. Chem. Phys. **103**, 10332–10346 (1995).

[27] M. A. Carignano and I. Szleifer, "Surface segregation in diblock copolymers and polymer blend thin films," Europhys. Lett. **30**, 525–530 (1995).

[28] G. H. Fredrickson, *The Equilibrium Theory of Inhomogeneous Polymers* (Oxford University Press, New York, 2006).

[29] N. Saitô, K. Takahashi, and Y. Yunoki, "The statistical mechanical theory of stiff chains," J. Phys. Soc. Jpn. **22**, 219–226 (1967).

[30] D. C. Morse and G. H. Fredrickson, "Semiflexible polymers near interfaces," Phys. Rev. Lett. **73**, 3235–3238 (1994).

[31] K. C. Daoulas, D. N. Theodorou, V. A. Harmandaris, N. C. Karayiannis, and V. G. Mavrantzas, "Self-consistent-field study of compressible semiflexible melts adsorbed on a solid substrate and comparison with atomistic simulations," Macromolecules **38**, 7134–7149 (2005).

[32] K. C. Daoulas, V. A. Harmandaris, and V. G. Mavrantzas, "Detailed atomistic simulation of a polymer melt/solid interface: Structure, density, and conformation of a thin film of polyethylene melt adsorbed on graphite," Macromolecules **38**, 5780–5795 (2005).

[33] A. V. Lukyanov and A. E. Likhtman, "Relaxation of surface tension in the free-surface boundary layer of simple Lennard-Jones liquids," J. Chem. Phys. **138**, 034712 (2013).

[34] D. G. Anderson, "Iterative procedures for nonlinear equations," J. Assoc. Comput. Mach. **12**, 547–560 (1965).

[35] V. A. Ivanov, A. S. Rodionova, J. A. Martemyanova, M. R. Stukan, M. Müller, W. Paul, and K. Binder, "Wall-induced orientational order in athermal semidilute solutions of semiflexible polymers: Monte Carlo simulations of a lattice model," J. Chem. Phys. **138**, 234903 (2013).

[36] S. K. Nath, J. D. McCoy, J. P. Donley, and J. G. Curro, "A modified self-consistent-field theory: Application to a homopolymer melt near a hard wall," J. Chem. Phys. **103**, 1635–1640 (1995).

[37] F. Schmid, "A self-consistent-field approach to surfaces of compressible polymer blends," J. Chem. Phys. **104**, 9191–9201 (1996).

[38] M. Müller and L. G. MacDowell, "Interface and surface properties of short polymers in solution: Monte Carlo simulations and self-consistent field theory," Macromolecules **33**, 3902–3923 (2000).

[39] M. Müller and L. G. MacDowell, "Short chains at surfaces and interfaces: A quantitative comparison between density-functional theories and Monte Carlo simulations," J. Chem. Phys. **118**, 2929–2940 (2003).

[40] A. Yethiraj, "Entropic and enthalpic surface segregation from blends of branched and linear polymers," Phys. Rev. Lett. **74**, 2018–2021 (1995).

[41] S. Tripathi and W. G. Chapman, "Microstructure and thermodynamics of inhomogeneous polymer blends and solutions," Phys. Rev. Lett. **94**, 087801 (2005).